Soil Biology & Biochemistry 111 (2017) 66–77

Contents lists available at ScienceDirect

Soil Biology & Biochemistry

journal homepage: www.elsevier.com/locate/soilbio

In-depth analysis of core methanogenic communities from high elevation permafrost-affected wetlands

Sizhong Yang [a, b, 1], Susanne Liebner [a, 1], Matthias Winkel [a], Mashal Alawi [a], Fabian Horn [a], Corina Dörfer [c], Julien Ollivier [d], Jin-sheng He [e, f], Huijun Jin [b], Peter Kühn [c], Michael Schloter [d], Thomas Scholten [c], Dirk Wagner [a, *]

[a] GFZ German Research Centre for Geosciences, Section 5.3 Geomicrobiology, Telegrafenberg, 14473 Potsdam, Germany
[b] State Key Laboratory of Frozen Soils Engineering, Northwest Institute of Eco-Environment and Resources, Chinese Academy of Sciences, 730000, Lanzhou, China
[c] University of Tübingen, Department of Geosciences, 72074 Tübingen, Germany
[d] Helmholtz Zentrum München, Research Unit Comparative Microbiome Analysis, 85764 Neuherberg, Germany
[e] Key Laboratory of Adaptation and Evolution of Plateau Biota, Northwest Institute of Plateau Biology, Chinese Academy of Sciences, 810008, Xi'ning, China
[f] Peking University, Department of Ecology, College of Urban and Environmental Sciences, 100871, Beijing, China

ARTICLE INFO

Article history:
Received 21 December 2016
Accepted 15 March 2017
Available online 7 April 2017

Keywords:
Methanogenic archaea
Wetland
mcrA gene
Frozen ground
Tibetan Plateau
Biogeography
Methanoregula

ABSTRACT

The organic carbon of permafrost affected soils is receiving particular attention with respect to its fate and potential feedback to global warming. The structural and activity changes of methanogenic communities in the degrading permafrost-affected wetlands on the Tibetan Plateau can serve as fundamental elements for modelling feedback interaction of ecosystems to climate change. Hence, we aimed at anticipating if and how the rapid environmental changes occurring especially on the high altitude Tibetan platform will affect methanogenic communities. We identified methanogenic community composition, activity and abundance in wetland soils with different hydrological settings, permafrost extent and soil properties and pinpoint the environmental controls. We show that despite a pronounced natural gradient, the Tibetan high elevation wetland soils host a large methanogenic core microbiome. Hydrogenotrophic methanogens, in particular *Methanoregula*, and H_2-dependent methanogenesis were overall dominant although acetoclastic methanogens in addition to hydrogenotrophs were among the dominating taxa in a minerotrophic fen. Tracing the *Methanoregula* community of the Tibetan Plateau using public databases revealed its global relevance in natural terrestrial habitats. Unlike the composition, the activity and abundance of methanogens varied strongly in the studied soils with higher values in alpine swamps than in alpine meadows. This study indicates that in the course of current wetland and permafrost degradation and the loss in soil moisture, a decrease in the methane production potential is expected on the high Tibetan Plateau but it will not lead to pronounced changes within the methanogenic community structure.

1. Introduction

The Qinghai-Tibet Plateau (QTP), also known as Tibetan Plateau, is the largest altitudinal permafrost unit on Earth. The lower elevation areas (<4000 m) are influenced by seasonally frozen ground, while on the high altitude plateau permafrost is more developed in depth, continuity and coverage (Zhou et al., 2000). The plateau is warming at a rate approximately two times higher than the global average since the 1950s (IPCC, 2007), and even faster at higher elevations (Wei and Fang, 2013). Permafrost degradation has occurred on the plateau during the last few decades, manifested by areal decrease of continuous and discontinuous permafrost, thinning of permafrost, shrinkage of isolated patches of permafrost and changes into seasonally frozen ground (Cheng and Wu, 2007; Jin et al., 2009; Wu et al., 2015). Around 18.6% of its permafrost has degraded in the past 30 years and up to 46% permafrost will disappear in 100 years (Cheng and Wu, 2007; Cheng and Jin, 2013). Degradation of permafrost has led to a

* Corresponding author.
E-mail address: dirk.wagner@gfz-potsdam.de (D. Wagner).
[1] Authors contributed equally to the manuscript.

http://dx.doi.org/10.1016/j.soilbio.2017.03.007

lowering of ground water levels, shrinking lakes and wetlands, and changes of grassland ecosystems from alpine meadows to steppes (Jin et al., 2009; Cheng and Jin, 2013).

Besides rivers and lakes, wetlands such as alpine swamps and meadows are fed mainly through precipitation and occur together with frozen ground. Alpine swamps and meadows occupy a large area of the eastern plateau (Zhou et al., 2000; Wang et al., 2016). While water in alpine meadows flows slowly through shallow flooded zones, the water in swamps is typically stagnant (Wang et al., 2016). The Tibetan wetlands altogether occupy 50% of the total wetland area of China (Ding and Cai, 2007), with the majority (85%) distributed in the headwater regions of the Yangtze and Yellow Rivers at higher elevations (>4000 m) and the Zoige (Ruoergai) Peat Plateau at lower altitudes (<4000 m; Zhang et al., 2011). It was estimated that 7.4 Pg C was stored at the top one meter of the whole alpine grasslands (Yang et al., 2008). Although there is no specific carbon estimate for the Tibetan wetlands, the soil organic density of wetlands was in general far higher than that of the alpine steppe and of the plateau's average, highlighting the alpine wetlands as important carbon pool with the potential for positive climate feedback (Ding and Cai, 2007; Yang et al., 2008; Ding et al., 2016). As a result of climate warming and permafrost degradation, the area of Tibetan wetlands reduced by about 8% from 1970 to 2006 (Zhao et al., 2015). Due to hydrological deterioration, degeneration from wetlands to meadows or from meadows to steppes have been observed at local scales (Jin et al., 2009; Brierley et al., 2016), which has subsequently impaired their roles in regulating the flow of rivers and carbon stores (Cheng and Jin, 2013).

The greenhouse gas methane is a major end product of the microbial degradation of organic matter under anaerobic conditions. Wetlands contribute 70% to the global total emission of methane and therefore are a major research focus (Bridgham et al., 2013). Moreover, ice core records showed that the variations in the atmospheric CH_4 content were consistent with the areal change of wetlands (Blunier et al., 1995). The methane fluxes on the Tibetan wetlands range from 9.6 to 214 mg CH_4 m^{-2} d^{-1} (Jin et al., 1999; Hirota et al., 2004; Cao et al., 2008; Chen et al., 2013) and are generally comparable to Arctic permafrost regions (Wille et al., 2008; Sachs et al., 2010; also see Fig. S1). Both alpine swamps and meadows are thus potential hotspot of methane emission on the plateau.

Methanogenic archaea (methanogens) are responsible for the biological production of methane (methanogenesis). They commonly use H_2/CO_2 (hydrogenotrophic) and acetate (acetoclastic) as substrates under anaerobic conditions (Wagner and Liebner, 2009). Methanogens on the Tibetan Plateau were studied in lakes (Liu et al., 2013) and wetland soils (Zhang et al., 2008; Deng et al., 2014; Cui et al., 2015; Tian et al., 2015). Most previous studies on wetlands were confined to the Zoige Plateau on the eastern margin of the plateau at lower elevation (3400–3600 m a.s.l.). In this region methanogenic community structure, in contrast to methane production, is little responsive to temperature increase and seasonal change (Cui et al., 2015). Methanogenic communities on swamps and meadows at the high plateau platform (>4000 m), however, remain poorly investigated despite their supposedly large relevance for the greenhouse gas (GHG) budget of the entire Tibetan Plateau. Also, anticipating if and how the rapid environmental changes presently occurring on the high Tibetan altitude platform will propagate into methanogenic communities is important.

This study is based on the assumption that methanogenic archaea respond to permafrost degradation, shrinkage of wetlands and extension of meadows. We expect that meadows differ from wetlands in displaying lower methanogenic activities and abundances, and significantly different composition in methanogenic communities. The objective of this research is to identify methanogenic community composition, activity and abundance in wetland soils with different hydrological settings (swamp and meadow), permafrost extent and soil properties, and to pinpoint the underlain environmental controls. Thereby, this study is the first to assess methanogenic communities on the Tibetan Plateau via deep sequencing on the functional gene of methanogenesis (methyl coenzyme M reductase A, *mcrA*) with a specific attention on the direct and indirect interactions between microbial taxa coexisting in the environment.

2. Material and methods

2.1. Study site and sample collection

The study sites on the northeastern Tibetan Plateau were selected along the air mass trajectory of the eastern Asian monsoon, by taking account of frozen ground, elevation and hydrology. Four sites were sampled in August 2012 when the active layer reached its maximum thaw depth: Huashixia (HUA), Donggi Cona Lake (DCL), Gande (GAN), and Haibei Station (HAI; Fig. 1). The variability of soil properties between each site was analyzed through a principal component analysis (PCA). Three of the sites are located above 4000 m while HAI is located at an elevation of approximately 3200 m similar to the Zoige wetland. HUA and DCL are located in the discontinuous permafrost region, whereas GAN and HAI are underlain by seasonally frozen ground (SFG). The sites DCL and HAI are swamp wetlands, while GAN and HUA are alpine meadows. For each research site, a series of soil profiles were described along an elevation gradient. The description of the HUA catena has been published recently (Dörfer et al., 2013). Of each catena, the profile which was most relevant for methanogenesis in terms of water level and soil moisture was selected for this study.

The DCL profile is located on a lakeshore wetland which derived from aeolian sediments. The sampling site at HUA is located on a patch of an alpine meadow near the Huashixia Permafrost Station. Laminated sandy or clayish sediments in yellowish and greyish were visible at this site where the discontinuous permafrost starts approximately at 80 cm below the surface. According to the Maduo climate station (98°12′ E, 34°54′ N, 4300 m a.s.l.) monitoring between 1953 and 2010, the mean annual air temperature (MAAT) near DCL and HUA is −4.1 °C with a mean annual precipitation (MAP) of 326 mm and most precipitation occurring in summer (280 mm, May to October). The GAN site is close to a small creek in a valley which is affected by deep seasonally frozen ground. The soil texture mainly consists of silt and clay. The MAAT at the GAN site is −2.2 °C, and the monthly average air temperature ranges from −15.2 °C (January) to 8.6 °C (July), with a MAP of around 550 mm in the period 1994 to 2010. Site HAI is a swamp affected by seasonally frozen ground where peat layer is visible in the entire profile. The MAAT at the Haibei weather station (37°29' - 37°45′N, 101°12' - 101°23′E, 2900–3500 m a.s.l.) is −1.7 °C with a maximum of 27.6 °C and a minimum of −37.1 °C in the period from 1989 to 2010. The MAP is around 500 mm with 80% within the growing season from May to September. The vegetation is generally dominated by sedges (*Kobresia* and *Carex*) with different coverage and density over different study sites.

At all study sites, soil profiles were excavated down to the permafrost table (approx. 50–70 cm) or to the water table (approx. up to 200 cm). After soil profile description, soil samples were taken in parallel for DNA extraction, methane production incubation and soil property analysis from the middle of each horizon. The samples were labeled with starting site name followed by increasing numbers indicating horizons from top to bottom, e.g.

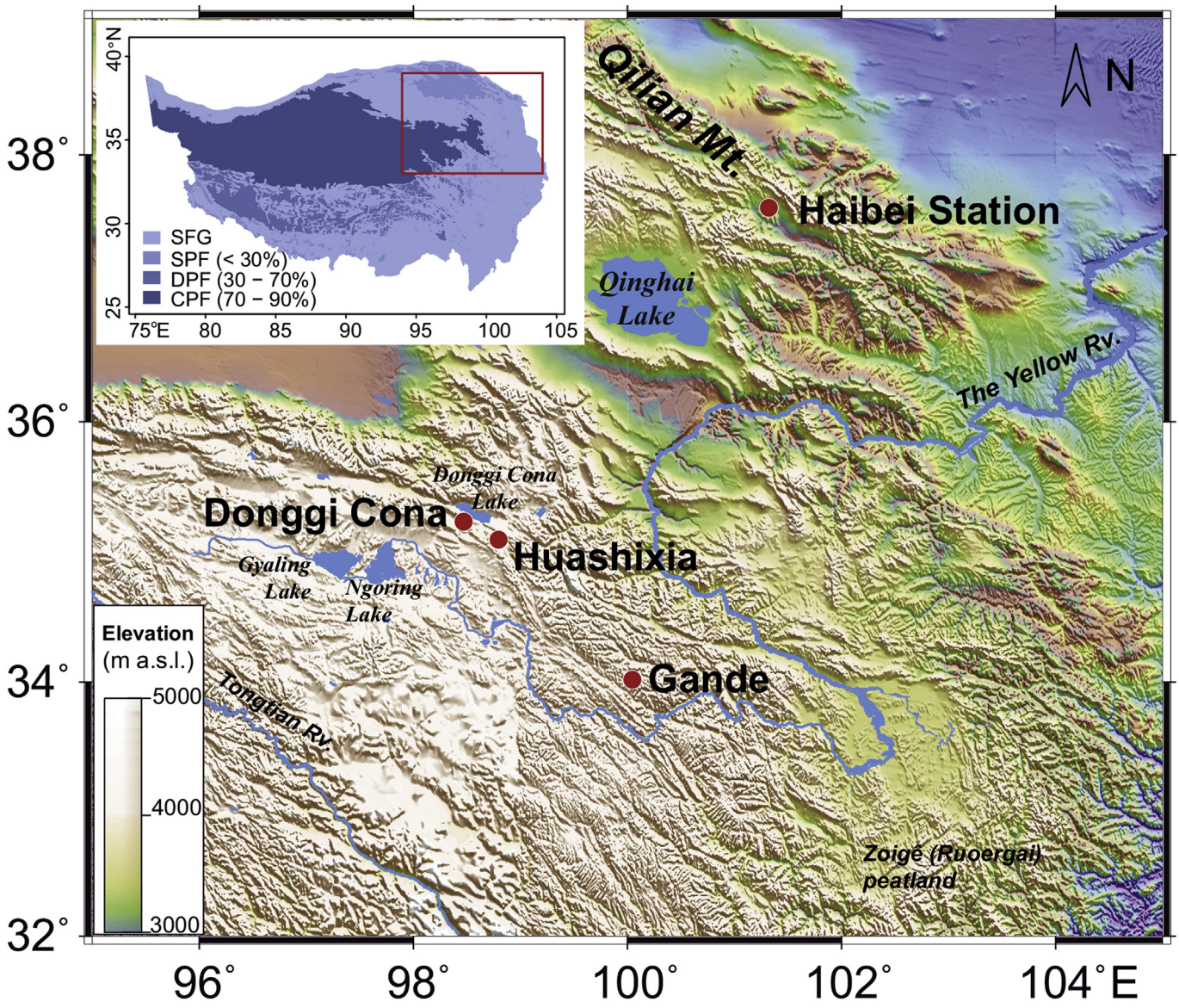

Fig. 1. Research sites in Qinghai province on the northeastern Qinghai-Tibet Plateau. The inset figure shows the frozen ground distribution on the plateau. The data is provided by Environmental and Ecological Science Data Center for West China, National Natural Science Foundation of China (http://westdc.westgis.ac.cn). The codes of SFG, SPF, DPF and CPF stand for seasonally frozen ground, sporadic permafrost, discontinuous permafrost and continuous permafrost, respectively. The red rectangle specifies the area in the enlarged map. Donggi Cona and Huashixia are located in discontinuous permafrost area, while Gande and Haibei Station are underlain by seasonally frozen ground. (For interpretation of the references to colour in this figure legend, the reader is referred to the web version of this article.)

DCL1, DCL2, DCL3 (Table S1). The soil properties for each depth were analyzed at the University of Tübingen according to the methods described by Dörfer et al. (2013). All soil chemical and physical parameters used in this study are listed in Table S1. Among these measures, calcium concentrations, in association with pH, overall have a large effect on the type of wetland that arises. These two factors are particularly important for the distinction between bogs and fens (Keddy, 2010).

2.2. Methane production rates

The samples were transferred into serum bottles in the lab and incubated in triplicates. Potential methane production rates were determined by gas chromatography as previously reported (Wagner et al., 2005). Briefly, fresh soil material (ca. 20 g) from different soil horizons was weighed into 100 ml glass jars in triplicates and closed with a rubber stopper. The samples were evacuated and flushed with ultrapure N_2. The headspace CH_4 concentration was determined over time by gas chromatography after adding 6 ml of sterile acetate solution (10 mM) or sterile and anoxic tap water in combination with H_2/CO_2 (80:20 v/v, 150 kPa). A sample without substrate served as control. The slurries were incubated at 10 °C according to the natural soil temperature regime. CH_4 production rates were calculated from the linear increase in CH_4 concentration over time.

2.3. DNA extraction and mcrA 454 amplicon sequencing

For logistic reasons, total soil DNA was immediately extracted in triplicates in the field using the FastDNA SPIN kit (MP Biomedicals,

Germany). The air-dried DNA was then stored on QIAsafe DNA 96-well filter plates (Qiagen, Germany) at ambient temperature according to the manufacturer instructions. In the lab, the DNA extract was dissolved from the filter and purified with the MiniElute PCR Purification Kit (Qiagen, Germany). In the course of a pilot shotgun sequencing of total DNA prior to this study, the DNA from the upper (top) and lower (down) horizons were pooled for HAI (HAI_t: 5 + 20 cm, HAI_d: 40 + 60 cm) and HUA (HUA_t: 5 + 15 cm, HUA_d: 35 + 55 cm) to obtain sufficient amounts of DNA. The *mcrA* fragment was amplified using the commonly-used primer set mlas and mcrA-rev. For multiplexing pyrosequencing, we used barcode-tagged forward and reverse primers at the 5′ end. PCR reactions were performed in triplicates in 50 μL reactions containing 1.0 μL DNA template (5–10 ng/μl) and 0.1 μM of each primer using the MangoMix PCR ready solution (Bioline GmbH, Berlin) according to the manufactor's manual. The PCR conditions were as follows: initial denaturation at 95 °C for 3 min; 30 cycles at 94 °C for 30 s, 55 °C for 45 s, and 72 °C for 45 s, with a final extension at 72 °C for 5 min. Afterwards, parallel PCR products for each sample were pooled and subsequently purified with the MiniElute PCR purification kit (Qiagen, Hilden, Germany). Pyrosequencing of the equalized mixture was performed on a Roche GS-FLX ++ Titanium platform at Eurofins Genomics (Germany). Sequencing of technical replicates showed highly reproducible results (Fig. S2).

2.4. Meta-data processing, alpha- and beta-diversity analysis

Raw sequences were processed by the mothur software package (v.1.31.2) (Schloss et al., 2009), following the standard operating procedure (https://www.mothur.org/wiki/454_SOP) with an additional frameshift check with FrameBot (see Table S2 for details). After fasta sequences were extracted from the raw sff sequence file in mothur, these sequences were first subjected to a translation check using the FrameBot tool (http://fungene.cme.msu.edu). Sequences with frameshift errors were excluded from further analysis with custom python script. The subsequent filtering removed the sequences with errors in barcodes or primers, homopolymers longer than 6 nucleotides, ambiguous bases, or average quality scores less than 25. Sequences shorter than 300 nucleotides or longer than 600 nucleotides were also discarded. The unique sequences were then aligned in mothur by default setting with referring to the pre-aligned *mcrA* sequences provided by the Fungene Pipeline database (http://fungene.cme.msu.edu). Chimeras were detected to be 7.7% of all the reads with the UCHIME algorithm by using the mothur software platform. Using the furthest neighbor clustering method in mothur, the valid sequences were assigned into operational taxonomic units (OTUs) at 84% identity of *mcrA* gene sequences (Yang et al., 2014). The abundance-based coverage estimator, Chao1 and Shannon estimator of species diversity, rarefaction curves and beta diversity metrics were calculated with *R* packages of vegan (v.2.0–7) (Oksanen et al., 2013) and phyloseq (v.1.10.0) (McMurdie and Holmes, 2013). For alpha diversity analysis, we avoided subsampling for the reasons given by McMurdie and Holmes (2014). For the beta diversity measures, the proportional abundance was used. We compared different normalization methods during the processing and found that the proportional standardization kept data features as close as possible to the original dataset and avoided the risk of overfitting our analysis (data not shown). The abundance variation of the major taxa across samples was visualized by bubble plot by using package ggplot2 v.1.0.0 (Wickham, 2009). The principal component analysis (PCA) was performed with the vegan package v.2.0–7 (Oksanen et al., 2013) and Venn diagrams were implemented in the VennDiagram package (Chen, 2013).

2.5. Quantitative PCR

Quantitative PCR was performed on a Bio-Rad CFX instrument (Bio-Rad, Munich, Germany) using the mlas/mcrA-rev primer pair. Different DNA template concentrations were tested to find the optimal dilutions avoiding inhibitions. The 25 μl reactions contained 12.5 μl of iTaq universal Sybr Green supermix (Bio-Rad, Munich, Germany), 0.25 μM concentrations of the primers, and 5 μl of diluted DNA template. The serial dilution of DNA standard from a *mcrA* clone (*M. barkeri*) ranged from 10^1 to 10^5 copies μl^{-1}. PCR was run by an initial denaturation for 10 min at 95 °C, followed by 40 cycles of denaturation at 95 °C for 30 s, annealing at 55° for 30 s, and extension at 72 °C for 45 s. Melt curve analysis was performed after the final extension by increasing the temperature from 50 to 95 °C at a ramp of 1.0 °C every 5 s. Each measurement was performed in triplicates, with R^2 of 0.994 and efficiency of 95%. The amount was given as copies per gram fresh soil.

2.6. Network construction

OTUs with average relative abundances less than 0.01% of the total number of OTU phylotypes were removed (Ma et al., 2016). Afterwards, we calculated all pairwise Spearman's rank correlations via *R* basic package (https://www.r-project.org/). The co-occurrence network was inferred based on the OTUs with a Spearman correlation coefficient (*rho*) > 0.6 and statistically significant p value < 0.01 (Barberan et al., 2012). This filtering step removed poorly represented OTUs and reduced network complexity, facilitating the determination of the methanogenic core community. The network was then generated by igraph package (v 1.0.1) (Csardi and Nepusz, 2006). The nodes in this network represent individual OTUs and the edges that connect these nodes represent correlations between OTUs. Community subgroups were detected via a walktrap modularity algorithm according to the internal ties and the pattern of ties between different groups.

2.7. Biogeography of dominant taxa

An integrated biogeography study was conducted to test the global relevance of the most dominant taxa among the high elevation Tibetan methanogens. Using representative sequences from our study, we searched for closely related sequences from the NCBI nucleotide database. Those sequences with identities higher than 84% according to the threshold by Yang et al. (2014) and the query coverage higher than 95% were recovered in the Genbank format. Afterwards, the corresponding PubMed accession numbers were used to track the original publications in order to bring focus on natural ecosystems by excluding the anthropogenic rice paddies and bioreactors. This effort ended up with 24 valid *mcrA* datasets globally. Then, the unique sequences for each library were phylogenetically assigned into different clades together with reference *mcrA* sequences of pure cultures. The incidence frequencies of sequences from each genus were calculated to compare their contribution to the overall diversity for each library. All these information was illustrated by a biogeographical map implemented by *R* packages of maptools (v.0.8–30) (Bivand and Lewin-Koh, 2014) and rgdal (v.0.9–1) (Bivand et al., 2014).

2.8. Phylogenetic tree construction

In order to have more precise taxonomic classification of the abundant OTUs, a phylogenetic tree was calculated based on representative sequences of each OTU (Fig. S3). The tree was inferred from representative sequences of a total of 25 OTUs having

a mean relative abundance higher than 1% across all libraries. These sequences with at least 400 nucleic acids were incorporated into a manually updated and curated reference ARB database to identify the closest relatives. Sequences of closely related environmental clones and cultured organisms together with the representative sequences were used for tree construction. A 30% base frequency filter was used to exclude highly variable positions. The phylogenetic tree was calculated using the neighbor-joining method and 1000 bootstrapped trials in ARB (http://www.arb-home.de/).

2.9. Statistical analysis

The similarity of community composition by sites was tested at genus levels with the function of 'adonis' in vegan package (Oksanen et al., 2013). The adonis function is to do permutational multivariate analysis of variance using distance matrices and is directly analogous to MANOVA. The subset of environmental variables which have the maximum (rank) correlation with community dissimilarities were identified with the 'envfit' function ($p < 0.05$) in vegan package. The environmental contribution to the community variations was further partitioned with partial constrained correspondence analysis (pCCA) through 'varpart' function in vegan package. For ANOVA analysis, the normality of data and homoscedasticity of variance by groups were firstly checked by the Shapiro-Wilk test and Bartlett's test, respectively. The Welch's one-way ANOVA was employed for heteroscedastic data with an unbalanced dataset or for balanced design with small sample sizes but very large variation in the standard deviations. Otherwise, the normal one-way ANOVA was used (McDonald, 2014). Following the co-occurrence network analysis, the abundance difference between different sites and the subgroups were tested by two-way ANOVA in *R* (https://www.r-project.org/).

The microbial community is generally not a random association, difference on abundance and occupancy due to niche differentiation can discriminate them as habitat generalists and specialists (Barberan et al., 2012). The generalists were selected by high incidence over samples and relative abundance, while the specialists were identified through indicator species (Logares et al., 2013). Indicator taxa of the study sites were assigned at genus level by using the labdsv package version 1.8–0 (Roberts, 2016) based on the indicator value (IndVal) index. The IndVal index combines the mean abundances of a taxon and its frequency of occurrence in all samples. A high indicator value is obtained by the combination of a large mean abundance of a taxon relative to others regions or habitats (specificity) and according to its presence in most samples of the same study site or habitat (fidelity) (Dufrene and Legendre, 1997).

2.10. Data deposition

The *mcrA* gene sequence data were deposited in the NCBI Sequence Read Archive (SRA) under the submission ID SRP046048.

3. Results

3.1. Characteristics of soils and sample sites

The correlation of all 13 soil variables (Table S1) with the two most important principal components is presented in Fig. 2. Two permafrost-affected sites DCL and HUA cluster closely. The other two sites HAI and GAN cluster separately from the permafrost sites. In addition, the deeper profile of GAN demonstrates a large vertical variability in contrast to the upper. The first principal component had high positive weightings from $CaCO_3$ content, salinity (in terms

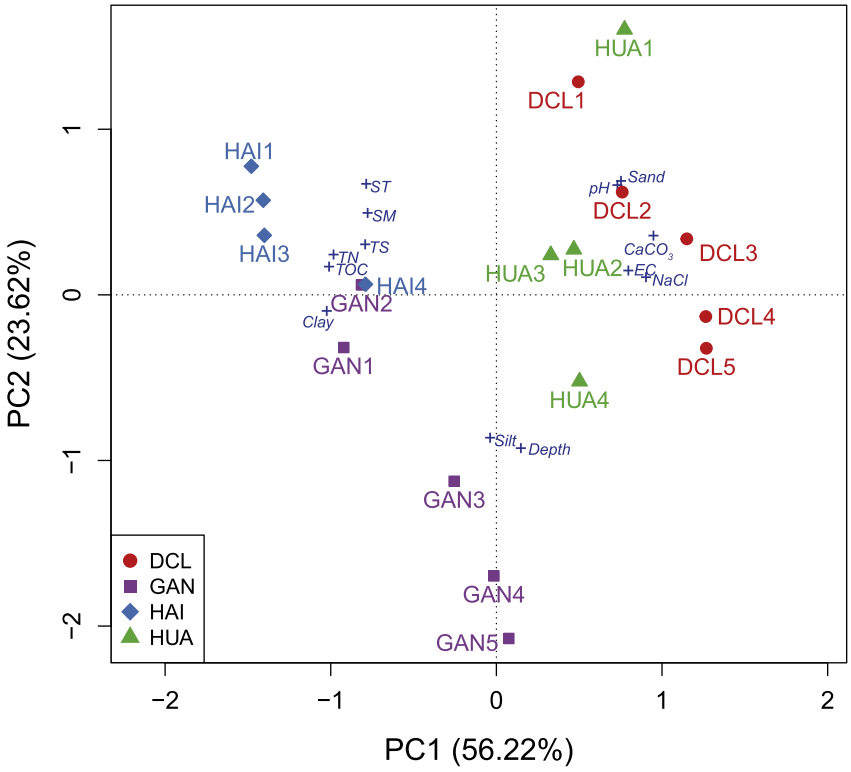

Fig. 2. PCA plot showing the variance of soil properties including sample depth, soil pH, total organic carbon (TOC), total nitrogen (TN), total sulfur (TS), $CaCO_3$ content, soil moisture (SM), soil temperature (SM), salinity (in terms of electric conductivity, EC), NaCl, soil texture parameters of silt, clay and sand content (please see Table S1 for details). Study sites: Donggi Cona (DCL), Gande (GAN), HAI (Haibei Station) and Huashixia (HUA). The study site numbers (e.g. 1, 2, 3 …) indicate the horizons from top to bottom.

of electric conductivity, EC), NaCl, pH and sand content. In contrast, variables of soils with high negative principal component 1 weightings were TOC, TN and clay content. These variables suggest that principal component 1 describes an alkalinity/pH axis. Interestingly, fertility, principally TOC and TN clumped with the soil alkalinity variables, which suggest it has a negative relationship with alkalinity/pH. The first and second axes explained 56.22% and 23.62% of the variance among sites, or 79.84% of the total variance. The first factor (alkalinity/pH) effectively separated two groups of wetlands: slightly acidic bogs at the left and more minerotrophic fen at the right. The silt content and depth along second axis are more related to the vertical variation of GAN profile.

3.2. Alpha-diversity

A total of 163,644 reads passed the quality filtering. The sequence counts ranged from 5797 to 18,290 per sample, except for upper layer samples of GAN (GAN1 and GAN2) which only yielded 1119 and 2702 reads, respectively. The number of OTUs, i.e. putative species richness is independent on the amount of reads in each library. The number of OTUs increased significantly within the first 500 reads, and gradually approached the saturation plateau after 2000 reads according to the rarefaction curves (Fig. S4). These sequences were assigned into a total of 175 OTUs including 40 singletons. A group of 25 dominant OTUs showed a mean relative abundance greater than 1% across all samples. These 25 OTUs accounted for 85.1% of the total reads while the remaining rare OTUs represented only 14.9% of the total. However, the rare OTUs fairly broaden the scope of biodiversity, leading to long tails in the rarefaction curves. The observed and estimated species richness was the highest in the DCL site while Shannon diversity indices peaked in HUA and HAI (Fig. S5). Alpha diversity was independent on hydrology, permafrost interior and soil depth.

3.3. Inter-site comparison of potential methane production, methanogenic abundance and beta-diversity

Differences in potential methanogenic activity and *mcrA* gene copy numbers between all samples are displayed in Fig. 3a and b. Thereby, methane production rates are shown for incubations both with acetate and with H_2/CO_2. References without added substrate are not shown because the rates were very low. In all samples, higher methane production rates were observed with H_2/CO_2 as substrate. The wetland-like samples from DCL and HAI exhibit the greatest potential methane production rates in comparison with the meadow samples of HUA and GAN. The maximum rates for the four sites are 15.8, 10.0, 1.0 and 3.3 nmol g^{-1} h^{-1} (Fig. 3a). The wetland samples also demonstrated higher *mcrA* gene copy numbers per gram fresh soils, with copy numbers up to 6.0–6.7 $\times$ 10^6 at DCL1 and DCL2 and 8.7 $\times$ 10^5 at HAI_t (Fig. 3b). However, the GAN samples characterized by low methane production rates showed peak gene copy numbers (6.0–7.6 $\times$ 10^5) overall comparable to the HAI wetland. Along the depth profiles of the wetland sites, the highest gene copy numbers occurred in the upper soil layers (6.7 $\times$ 10^6 at DCL2 and 8.7 $\times$ 10^5 at HAI_t), while the gene copy numbers along the two meadow profiles (HUA and GAN) were greater in the lower soil layers (7.6 $\times$ 10^5 at GAN3 and 4.2 $\times$ 10^5 at HUA_d).

The compositional heterogeneity of the dominant methanogenic taxa at the genus level was shown by a bubble plot for the depth profiles of each site (Fig. 3c). The taxonomic affiliation of the 25 dominant OTUs (relative abundances >1%) is displayed in Fig. S3. The lineages along vertical axis correspond to the decreasing rank of their mean relative abundance. Five genera namely *Methanobacterium*, *Methanomassiliicoccus*, *Methanoregula*, *Methanosaeta* and *Methanosarcina* exist throughout all sites, but with relative abundance varying with sites and along the vertical profiles of each site. Among them, *Methanoregula* is not only the most abundant but also the most diverse genotype, with 11 different OTUs identified (Table 1). *Methanomassiliicoccus* ranks as the second most abundant and diverse. Members of the facultative acetoclastic genus *Methanosarcina* and the obligate acetoclastic genus *Methanosaeta* exhibit reverse proportion between DCL and HAI or HUA, respectively. In general, *Methanosarcina* displays in a pattern opposite to *Methanoregula*. *Methanosaeta* exists with lesser relative abundances with the exception in the sample GAN2 (20 cm). According to the IndVal indices (Table 2), *Methanobacterium*, *Methanosarcina* and *Methanospirillum* are identified as indicator (specialist) taxa for the site DCL and *Methanoflorens* for the HAI site (IndVal $p < 0.05$). The major difference in community composition on the genus level was observed between the two wetland sites DCL and HAI, although there is not enough evidence that the community compositions at genus level are statistically different by sites according to adonis analysis ($p = 0.15$).

To further disentangle differences in methanogenic community composition between the study sites and to verify whether the conclusions drawn on the genus level also hold on the species level, co-occurrence patterns and shared OTUs were identified (Fig. 4). Eighty OTUs with Spearman's *rho* > 0.6 and $p < 0.01$ out of 175 total OTUs were selected for network analysis (Table S3). The network consists of 80 nodes (OTUs). Three subgroups were detected according to the internal ties as well as the pattern of ties between different groups (Fig. 4a). Subgroup 1 contains 53 OTUs (nodes) and is represented by the most abundant OTUs, while subgroup 2 with 22 nodes is mainly composed of less dominant groups. Within subgroup 2, the top 3 abundant OTUs belong to *Methanoregula*, *Methanosaeta* and *Methanosarcina*. Subgroup 3 only contains five OTUs and represents the generalists among the group of rare OTUs. The two large subgroups altogether account for 89.5% of all sequences. The two-way ANOVA test indicates that the effect of community subgroups is statistically significant ($p < 0.001$) while there is not enough evidence showing that the influences of the study site ($p = 0.484$) and the interaction between the two factors ($p = 0.135$) are significant. Increasing the correlation coefficient from 0.6 to 0.8 still revealed an insignificant influence of the study site highlighting the robustness of this finding. Fig. 4b displays the interaction in a two-way ANOVA, presenting the mean relative abundance per OTU for each subgroup at each site. According to this network analysis and consistency with Fig. 3c and Table 2, the main community shifts at both the genus and putative species levels occur between the two wetland sites DCL and HAI. At the same time, the network analysis and the bubble plot in Fig. 3 point at a large core methanogenic biome of all sites irrespective of whether they display a pronounced or low methane production. This finding is supported by the Venn diagram (Fig. 4c) showing the presence and absence of OTUs with a relative abundance above 1%. This result highlights a large share of species between all sites coinciding with group 1 of the network analysis which is highly abundant in all sites.

The variation of methanogenic communities was statistically correlated with a subset of 7 environmental variables ($p < 0.05$). In general, variables associated with soil alkalinity and salinity properties (including $CaCO_3$ content; pH; sand content; electrical conductivity, EC; and NaCl) point towards the DCL cluster, while those associated with soil fertility (*i.e.* TOC and TN) point towards the other sites (Fig. S6). The pCCA result indicated that approximately 62.8% of the total variation could be explained by this subset of environmental variables. Soil alkalinity plus salinity and soil fertility can explain 39.1% and 14.3% of the total variation in the data set, respectively, with 9.4% shared partition (intersection) by both

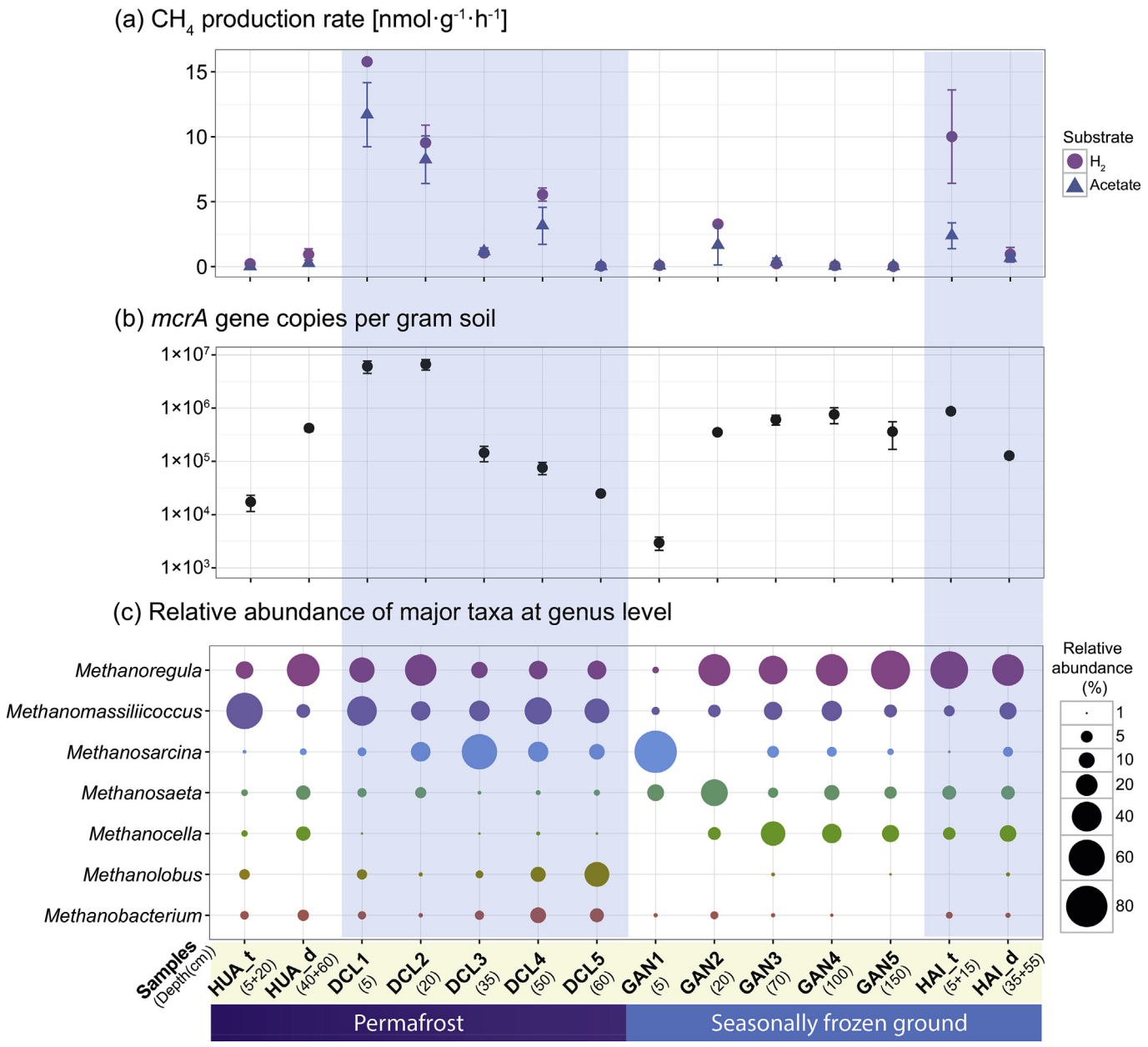

Fig. 3. Comparison of potential methane production (a), methanogenic abundance (b) and methanogenic community composition on genus level (c) of each sample. In Fig. 3b, the y axis is transformed by $\log_{10}$, and thus leading to disproportional length of the upper and lower error bar for each point. HUA, DCL, GAN and HAI represent study sites of Huashixia, Donggi Cona Lake region, Gande and Haibei Station, respectively. Following the sites HUA or HAI are the tags 't' and 'd' indicating the merged samples for the 'top' and 'deep' layers for those two profiles. The blue background indicates swamp wetlands while the white background indicates alpine meadows. (For interpretation of the references to colour in this figure legend, the reader is referred to the web version of this article.)

Table 1
The absolute and relative sequence frequencies of the most abundant OTUs which have a mean relative abundance >1% across samples at genus level.

Lineage	No. of OTUs	No. of reads	% in total valid reads
Methanoregula	11	56,150	34.68
Methanomassiliicoccus	4	36,086	18.73
Methanosarcina	2	18,457	14.48
Methanosaeta	4	6760	6.7
Methanocella	2	10,483	6.15
Methanolobus	1	6986	3.26
Methanobacterium	1	4217	2.38

factors (Fig. S7).

3.4. Global occurrence of methanoregula sequences

The genus *Methanoregula* was observed as the top diverse and abundant lineage across all studied high elevation Tibetan soils and was therefore selected for a meta-study on its biogeography in 24 globally-distributed libraries. Members of the *Methanoregula*-community of the high elevation Tibetan plateau were found occurring at diverse geographical locations, covering a variety of habitats including wetland, peatland, fen, bog, forest and grassland soils, lakes, riparians, estuaries and subglacial sediments (Fig. 5, Table S4). Among them, wetlands account for the largest proportion

Table 2
Indicator taxa for different sites according to indicator value (IndVal index). The IndVal index combines species mean abundances and its frequencies of occurrence in the groups. A high indicator value is obtained by a combination of large mean abundance within a group compared to the other groups (specificity) and presence in most samples of that group (fidelity). Taxa with $p < 0.05$ were identified as indicator species. Frequency demonstrates the total number of samples upon which a given indicator taxon occurs. DCL, GAN, HAI and HUA represent the study sites of Donggi Cona Lake region, Gande, Haibei Station and Huashixia, respectively.

Genera	IndVal	*p* value	Frequency	Sites
Methanobacterium	0.6035	0.029*	14	DCL
Methanobrevibacter	0.6291	0.130	5	DCL
Methanocella	0.4172	0.659	12	GAN
Methanoculleus	0.4000	0.455	2	DCL
Methanoflorens	0.9328	0.019*	9	HAI
Methanofollis	0.7257	0.107	8	DCL
Methanolinea	0.2000	1.000	1	DCL
Methanolobus	0.8386	0.054	9	DCL
Methanomassiliicoccus	0.4219	0.370	14	DCL
Methanomethylophilus	0.3969	0.374	6	DCL
Methanomethylovorans	0.8358	0.114	8	HUA
Methanoregula	0.3243	0.730	14	HAI
Methanosaeta	0.3912	0.298	14	HAI
Methanosarcina	0.7420	0.013*	14	DCL
Methanosphaerula	0.1938	0.975	7	DCL
Methanospirillum	0.7303	0.030*	10	DCL

(ca. 51%) in comparison to other ecosystems. More importantly, members of the *Methanoregula* lineage appear to dominate the overall methanogenic diversity in most of the sites (Fig. 5). Welch's ANOVA suggest that the incidence frequencies of *Methanoregula* are statistically different to the other genera ($p < 0.001$, Fig. S8).

4. Discussion

The turnover of organic matter in permafrost environments is mainly driven by microbial communities and their activity under given *in situ* conditions. Nevertheless, the reaction of microbial communities to changing environmental conditions in frozen-ground-affected soils is still an unknown variable in the climate change equation (Graham et al., 2012). High elevation soils on the Tibetan Plateau are characterized by young development, frequent polygenetic formation and strong degradation features which are affected by cryogenic or erosive processes (Baumann et al., 2009). The presented results revealed that the degradation of wetlands and permafrost lead to a decrease in the methane production potential on the Tibetan Plateau without pronounced changes in the community structure of methanogenic archaea.

The methanogenic communities in the investigated soils at the Tibetan high elevation are dominated by hydrogenotrophic rather than acetoclastic methanogens, which is in agreement with higher methane production rates in the presence of H_2/CO_2 compared with acetate as substrate. For bog-like wetlands such as HAI, low pH generally limits acetotrophic in favor of hydrogenotrophic methanogenic metabolism (Kotsyurbenko et al., 2007; Bridgham et al., 2013). In contrast to the low pH at HAI, the relative abundance of major taxa (Fig. 3c) shows a greater occurrence of the acetoclastic genera *Methanosarcina* and lower abundance of hydrogenotrophic methanogens such as *Methanoregula* at high pH values as observed

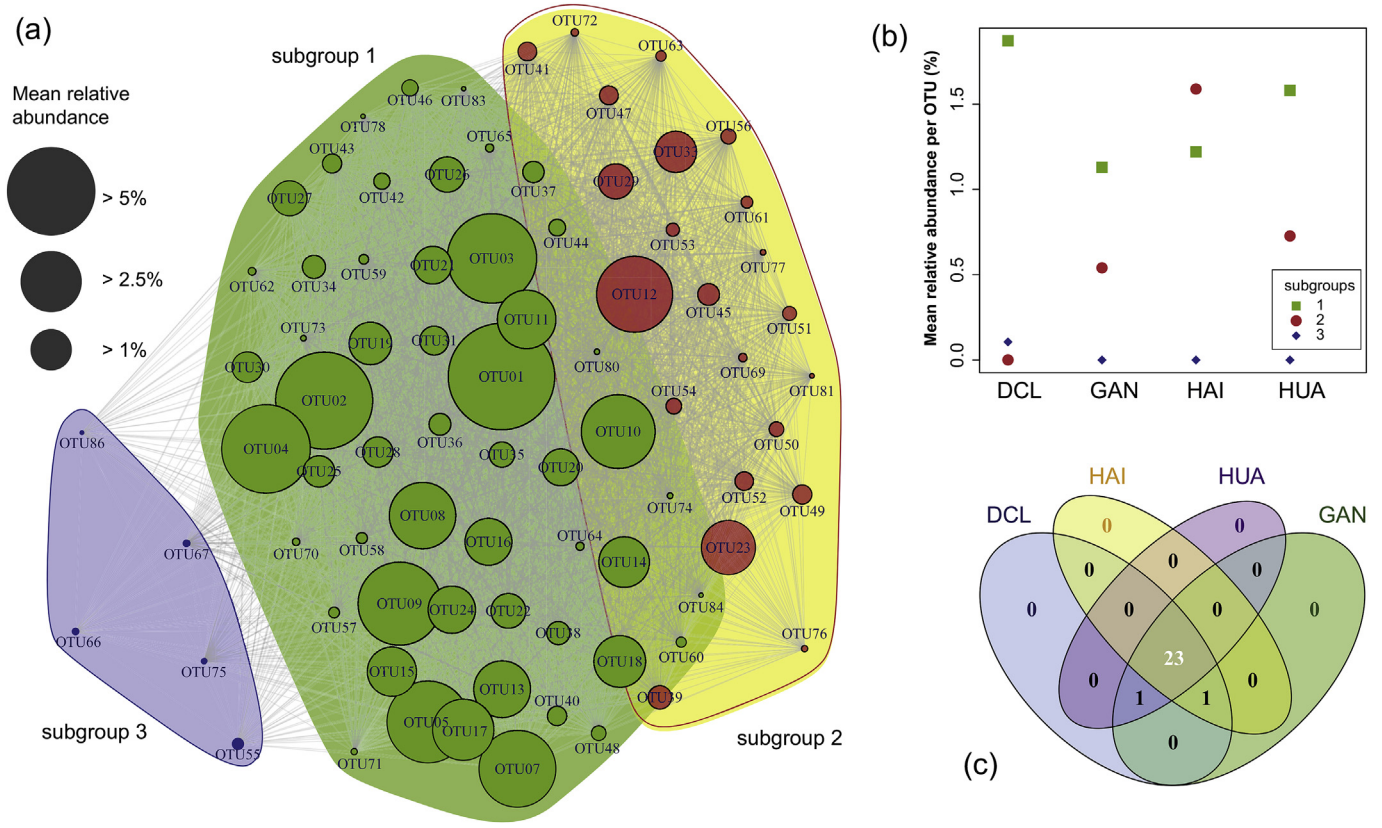

Fig. 4. Community shift on OTUs level. A total of 80 OTUs were used for valid network analysis in Fig. 4a. The subgroups were identified by the walktrap algorithm with igraph package. The node colors of green, red and blue correspond to the subgroup 1, 2 and 3. The size of nodes corresponds to the mean relative abundance of that OTU across all samples. Fig. 4b displays the interaction between the community subgroups and different sites on the mean relative abundance per OTU phylotype. In Fig. 4c, the shared OTUs were based on the relatively abundant OTUs with mean relative abundance >1% throughout all samples. (For interpretation of the references to colour in this figure legend, the reader is referred to the web version of this article.)

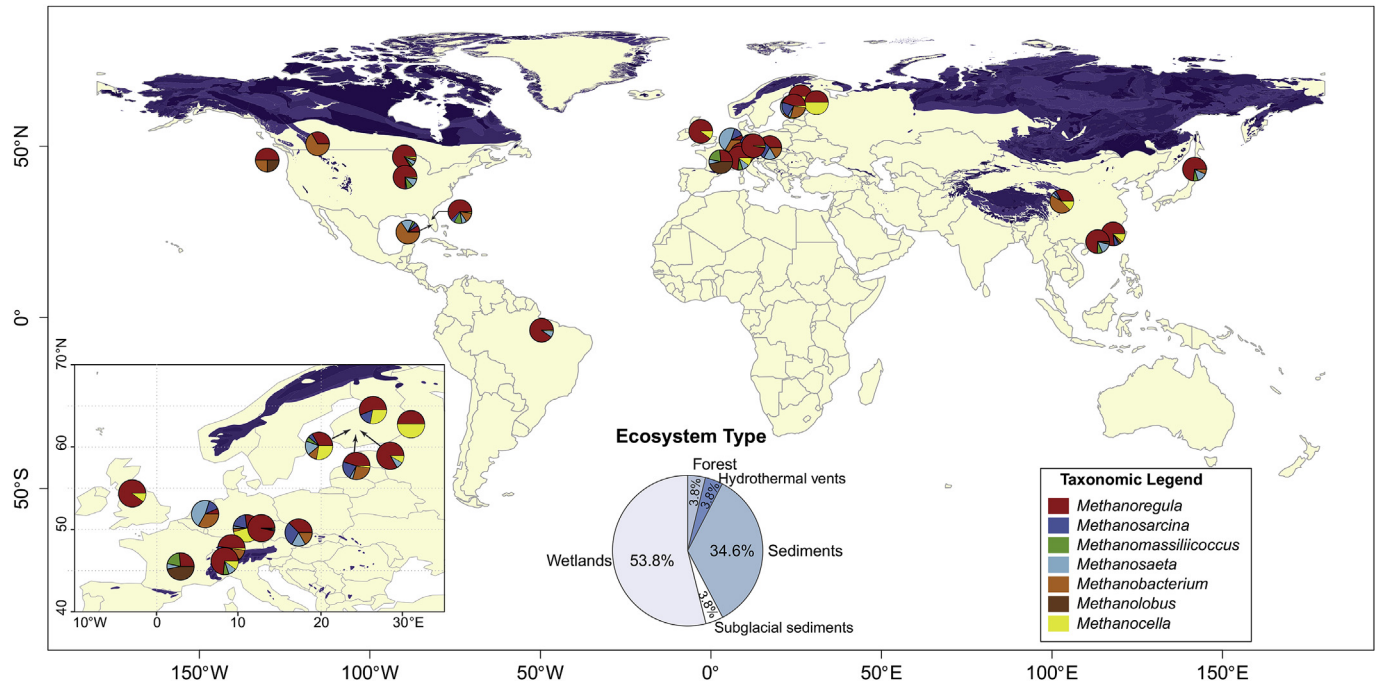

Fig. 5. Global occurrence of *Methanoregula*-like sequences. Each pie chart represents an instance where one or more published *mcrA* nucleotide sequences with >84% identity to the representative sequences of the OTUs from our Tibetan libraries which were assigned to the genus of *Methanoregula*. On the biogeography map are 24 pie charts showing the contribution of each genus to the overall diversity of each library. Colors inside the pie chart were coded according to taxonomic groups. Since the European sites are too dense, an inset figure is used to enlarge the display. For the permafrost, different purple colors represent different permafrost distribution and classification. The permafrost data was retrieved from http://nsidc.org/data/docs/fgdc/ggd318_map_circumarctic/(National Snow and Ice Data Center). (For interpretation of the references to colour in this figure legend, the reader is referred to the web version of this article.)

at DCL. However, pH difference alone are insufficient to explain the relative importance of the two pathways of methanogenesis (Bridgham et al., 2013), which means that other environmental factors also control the balance of the two major pathways of methanogenesis in wetlands of the Tibetan Plateau. Most of the natural wetlands such as bogs and fens have low H_2 partial pressures (Conrad, 1999; Sakai et al., 2009). Under these conditions, acetate will be converted into H_2 and CO_2 by syntrophic acetate-oxidizing bacteria coupled with hydrogen-dependent methanogenesis (Hattori, 2008; Thauer et al., 2008). Even if it was shown by Kotsyurbenko (2005) that homoacetogens during syntrophic glucose degradation at low temperatures are able to utilize H_2 at a slightly higher rate compared to methanogenic archaea, in case of low hydrogen concentrations H_2-utilizing methanogens successfully outcompete homoacetogenic bacteria. Evidence also exists that low temperatures favor the use of H_2/CO_2 over acetate by methanogens (Nozhevnikova et al., 1994). In addition, the facultative acetoclastic order *Methanosarcinales* possesses cytochromes and requires a H_2 pressure at least tenfold higher than other methanogens without cytochromes, and are thus likely to be outcompeted under low H_2 partial pressures (Thauer et al., 2008). These genetic, metabolic, and thermodynamic traits may render competing advantage to the hydrogenotrophic methanogens under low H_2 partial pressure, which prevail in many natural terrestrial habitats (Conrad, 1999; Thauer et al., 2008) and is expected to occur on the Tibetan Plateau as well, given the low air pressure at high altitudes.

The methane production activity in different soil ecosystems on the Tibetan Plateau is another important aspect to understand the anaerobic carbon dynamics under changing environmental conditions. The large abundance of methanogens and the higher potential activity observed in the swamp wetlands in contrast to alpine meadows suggests a potential loss in methanogenic activity in the event of on-going deterioration of wetlands and permafrost on the Tibetan Plateau. Our study is, however, restricted to the DNA level and might therefore underestimate or overestimate the active methanogenic community which would be better described through an RNA approach (Freitag and Prosser, 2009). This includes changes not only in the hydrological conditions but also in the quality and availability of soil organic matter (Wagner et al., 2005; Wagner et al., 2009). At DCL, for example, the observed high methanogenic activity is rather contrasting the low TOC content. Like many minerotrophic fen patches in the alpine headwater regions of Yangtze and Yellow Rivers, the calciphilous soil at DCL is little developed and lacks solid TOC. It is the water supply from lakes or rivers, which leads to the development into minerotrophic wetlands. In minerotrophic fens, abundant labile and high-quality plant material can stimulate CH_4 emissions via the acetoclastic pathway (Megonigal et al., 2005; Bridgham et al., 2013). Consistently, the proportion of acetoclastic *Methanosarcina* species increases in the rhizosphere horizon of DCL (Fig. 3c). A high proportion of *Methanosarcinales*-related methanogens was also reported for the Zoige wetland (Zhang et al., 2008). However, the better availability of acetate at DCL does not necessarily mean acetotrophic methanogenesis will dominate methane production. Results from Alaskan wetlands also showed the dominance of hydrogenotrophic rather than acetoclastic methanogenesis even though acetate substantially accumulated in these soils (Rooney-Varga et al., 2007). Also, acetate can be converted to CO_2 which eventually increases the relative contribution of H_2 dependent methanogenesis (Duddleston et al., 2002). On the other hand, CO_2 and CH_4 from anaerobic respiration in bogs are derived from a combination of dissolved organic matter (DOM) and the bulk peat (Megonigal et al., 2005; Chanton et al., 2008). Despite plant exudates are released to the anaerobic peat layers of the bog wetlands at HAI, the recalcitrant old peat is the main carbon source for

methanogenesis (Bridgham et al., 2013). The size of labile organic matter is overall smaller leading to lower CH_4 production rates in HAI compared to DCL. Finally, the on-going rapid wetland and permafrost degradation tends to substantially deteriorate the moisture regime of the marginal sandy patches of minerotrophic fens as for instance at DCL, which will reduce the methane production in these wetlands.

Comparing alpha-diversity measures with methane production and methanogenic abundance revealed that even samples with low methane production activity are characterized by a comparably high alpha-diversity (Fig. S5). The diversity of the genomic pool of methanogens appears thus independent from methane production rates and methanogenic abundances at least when excluding the very rare taxa. Also, taxa such as *Methanoregula*, *Methanomassiliicoccus* and *Methanosaeta* prevail throughout all samples, and may constitute Tibetan high elevation keystone species. Particularly, the hydrogenotrophic *Methanoregula* species were frequently observed prevalent in various habitats (Galand et al., 2005; Bräuer et al., 2006) including the Tibetan Zoige wetland (Zhang et al., 2008), a comparable wetland to the HAI wetland of this study. The global distribution of *Methanoregula* sequences further demonstrates that this lineage is successful in a diverse set of environments as mentioned above, and can be considered a generalist taxon in natural terrestrial habitats. Additionally, the H_2-dependent methylotrophic genus *Methanomassiliicoccus* is an abundant group throughout all samples. This lineage was newly re-evaluated and shown to be widespread in the environment, with at least two distinctive phylogenetic clades in wetlands and animal guts, respectively (Sollinger et al., 2016). The prevalence of *Methanomassiliicoccus* related sequences in this study indicate an important but potentially overlooked role in methane production, which needs further investigation.

By the detailed analysis of the *mcrA* sequences it was further possible to identify a number of indicator species. By definition, an indicator species is an organism whose presence reflects a specific environmental condition (Dufrene and Legendre, 1997). Currently, the lineage *Methanoflorens* was newly proposed as methanogenic indicator species of acidic peatlands exposed to thawing permafrost (Mondav et al., 2014). This species was also identified as indicator species for the bog wetland at HAI. The seasonally frozen ground at this site, which was characterized by sporadic permafrost during the little ice age (Cheng and Jin, 2013), can be regarded as degraded permafrost. This may serve as an explanation for the specific occurrence of *Methanoflorens* at the HAI site where permafrost has degraded into seasonally frozen ground (Fig. 3b). Furthermore, a total of three indicator species (*Methanobacterium*, *Methanosarcina* and *Methanospirillum*) were identified for DCL by analyzing the indicator value index (IndVal), highlighting the distinction of this minerotrophic wetland. This minerotrophic fen characterized by high alkalinity/pH, salinity and little-developed calciphilous soil appears to have a distinct methanogenic community differing in the relative proportion of methanogenic taxa from that of bogs on the Tibetan Plateau.

In addition to alpha- and beta-diversity analysis we exploited network analysis for identifying co-occurrence patterns which can provide insights about patterns of potential biotic interactions, shared physiologies and habitat affinities (Barberan et al., 2012). The three Tibetan community subgroups that we identified assemble independent of the study sites and thus geographic location according to two-way ANOVA. Subgroup 1 of the network analysis includes the most abundant OTUs while subgroup 2 is generally composed of a suite of sub-abundant OTUs. In the bog wetland of HAI, subgroup 2 outcompeted the subgroup 1. This means that the network analysis highlights differences in community composition on the species level between the wetland types, which emerge already when comparing the communities on the genus level (Fig. 3c). Despite compositional changes in terms of relative abundances of methanogens especially between the two wetlands, the two large subgroups identified illustrate a large core of methanogenic associations contributing almost 90% to the total methanogenic abundance in all study sites. A large methanogenic core biome irrespective of permafrost conditions and methane production potential is supported through the analyses of shared OTUs (Fig. 4c) illustrating that among the 25 most abundant OTUs, 23 occur in all study sites.

The spatial variations in methanogenic communities in the studied wetlands on the Tibetan Plateau are regulated by different factors of soil properties for different wetland types. The fertility (TOC and TN), which is the main determinant in the bog, are in contrast to the alkalinity and salinity factors for the minerotrophic fen of DCL. This result implies that the organic matter accumulates in the DCL fen are less determinative for the community composition than in the bog, which are presumably fueled by fresh plant material (Megonigal et al., 2005; Bridgham et al., 2013). Moreover, the importance of TOC and TN for methanogens in the HAI site is in line with the constraint of organic quality for methanogens in bogs (Megonigal et al., 2005; Chanton et al., 2008; Bridgham et al., 2013). For Tibetan soils, the status of $CaCO_3$ content and pH indicate the maturity stage of pedogenesis. The initially formed soils with high pH values and carbonate contents generally exhibit extremely low contents of deposited C and N (Baumann et al., 2009). That is why the fertility and alkalinity are negatively correlated along the first principal component. In addition, approximately 37.2% variations in the communities cannot be explained by the studied environmental parameters, and other factors should be taken into account for interpreting the community differences, such as above and below ground biomass, plant species composition, and syntrophic microorganisms (e.g., homoacetegens) involved in the fermentation processes.

To the best of our knowledge, this study is the first conducting research on methanogens of the high elevation wetland soils on the Tibetan Plateau. Here we show that on the high elevation plateau, the potential methane production and abundance of methanogens varies between swamp wetlands and alpine meadows with highest rates of methane production in minerotrophic fen-like wetlands, whilst the underlain extent of permafrost may exert a more indirect influence on the methanogens by regulating hydrological and temperature regimes. This finding contrast with previous studies suggesting substantial alterations of the methanogenic community with permafrost thawing (Hodgkins et al., 2014; McCalley et al., 2014; Liebner et al., 2015), but support others showing no significant change in the relative contribution of the two predominant methangenic pathways in Arctic systems (Prater et al., 2007). The methanogenic communities in the studied Tibetan wetland soils appears to be represented by a substantial core assemblage of methanogenic taxa probably due to distinctive environmental conditions prevailing on the Tibetan high altitude environments such as low partial pressures of H_2, low precipitation, and comparably young and little developed soils. Hydrogenotrophic methanogens (especially *Methanoregula*) generally prevail across the wetland and wet-meadow sites and H_2-dependent methanogenesis is the major pathway in the studied soils on the Tibetan Plateau. Facing the degradation of wetlands and permafrost and the loss in soil moisture as a consequence of global change, the methane production potential is likely to be more constrained in the patches of shallow sandy minerotrophic fens on the headwater regions of the high Tibetan Plateau due to their hydrological and nutritious vulnerability. Based on this study we show that the methanogenic community structure in general will not change drastically, even if the relative abundance of acetotrophic

methanogens that thrive in some wetland environments may potentially decrease. The dominance of hydrogenotrophic methanogens will presumably persist or even increase in these wetland types.

Acknowledgements

The authors wish to thank the Chinese-German field parties during the field expedition 2012, especially Dr. Mi Zhang (Northwest Institute of Plateau Biology, CAS), Prof. Yongzhi Liu, Dr. Ji Chen and Prof. Qingbai Wu (Northwest Institute of Eco-Environment and Resources, CAS). We would like to thank Arwyn Edwards (Aberystwyth University) and one anonymous reviewer for their helpful suggestions and comments. This work was supported by the German Federal Ministry of Education and Research (BMBF) in the framework of the BMBF program 'WTZ Central Asia - Monsoon Dynamics and Geo-ecosystems' by grants to DW [grant number 03G0810B], MS [grant number 03G0810C] and TS [grant number 03G0810A]. It was also supported by the Helmholtz Association (HGF) by funding the Helmholtz Young Investigators Group of SL [VH-NG-919].

Appendix A. Supplementary data

Supplementary data related to this article can be found at http://dx.doi.org/10.1016/j.soilbio.2017.03.007.

References

Barberan, A., Bates, S.T., Casamayor, E.O., Fierer, N., 2012. Using network analysis to explore co-occurrence patterns in soil microbial communities. ISME Journal 6, 343–351.

Baumann, F., He, J.S., Schmidt, K., Kuhn, P., Scholten, T., 2009. Pedogenesis, permafrost, and soil moisture as controlling factors for soil nitrogen and carbon contents across the Tibetan Plateau. Global Change Biology 15, 3001–3017.

Bivand, R., Keitt, T., Rowlingson, B., 2014. Rgdal: bindings for the Geospatial Data Abstraction Library. R package version 0.9-1. http://CRAN.R-project.org/package=rgdal.

Bivand, R., Lewin-Koh, N., 2014. Maptools: Tools for Reading and Handling Spatial Objects. R package version 0.8-30. http://CRAN.R-project.org/package=maptools.

Blunier, T., Chappellaz, J., Schwander, J., Stauffer, B., Raynaud, D., 1995. Variations in atmospheric methane concentration during the Holocene epoch. Nature 374, 46–49.

Bräuer, S.L., Cadillo-Quiroz, H., Yashiro, E., Yavitt, J.B., Zinder, S.H., 2006. Isolation of a novel acidiphilic methanogen from an acidic peat bog. Nature 442, 192–194.

Bridgham, S.D., Cadillo-Quiroz, H., Keller, J.K., Zhuang, Q., 2013. Methane emissions from wetlands: biogeochemical, microbial, and modeling perspectives from local to global scales. Global Change Biology 19, 1325–1346.

Brierley, G.J., Li, X., Cullum, C., Gao, J., 2016. Landscape and Ecosystem Diversity, Dynamics and Management in the Yellow River Source Zone. Springer, Switzerland.

Cao, G., Xu, X., Long, R., Wang, Q., Wang, C., Du, Y., Zhao, X., 2008. Methane emissions by alpine plant communities in the Qinghai-Tibet Plateau. Biology Letters 4, 681–684.

Chanton, J.P., Glaser, P.H., Chasar, L.S., Burdige, D.J., Hines, M.E., Siegel, D.I., Tremblay, L.B., Cooper, W.T., 2008. Radiocarbon evidence for the importance of surface vegetation on fermentation and methanogenesis in contrasting types of boreal peatlands. Global Biogeochemical Cycles 22, GB4022.

Chen, H., Wu, N., Wang, Y., Zhu, D., Zhu, Q.a., Yang, G., Gao, Y., Fang, X., Wang, X., Peng, C., 2013. Inter-annual variations of methane emission from an open fen on the Qinghai-Tibetan plateau: a three-year study. Plos One 8, e53878.

Chen, H.B., 2013. VennDiagram: Generate High-resolution Venn and Euler Plots. R package version 1.6.0. http://CRAN.R-project.org/package=VennDiagram.

Cheng, G.D., Jin, H.J., 2013. Permafrost and groundwater on the Qinghai-Tibet Plateau and in Northeast China. Hydrogeology Journal 21, 5–23.

Cheng, G.D., Wu, T.H., 2007. Responses of permafrost to climate change and their environmental significance, Qinghai-Tibet Plateau. Journal of Geophysical Research-Earth Surface 112, F02S03.

Conrad, R., 1999. Contribution of hydrogen to methane production and control of hydrogen concentrations in methanogenic soils and sediments. FEMS Microbiology Ecology 28, 193–202.

Csardi, G., Nepusz, T., 2006. The igraph software package for complex network research. InterJournal. Complex Systems 1695. 2006. http://igraph.org.

Cui, M.M., Ma, A.Z., Qi, H.Y., Zhuang, X.L., Zhuang, G.Q., Zhao, G.H., 2015. Warmer temperature accelerates methane emissions from the Zoige wetland on the Tibetan Plateau without changing methanogenic community composition. Scientific Reports 5, 11616.

Deng, Y.C., Cui, X.Y., Hernandez, M., Dumont, M.G., 2014. Microbial diversity in hummock and hollow soils of three wetlands on the Qinghai-Tibetan Plateau revealed by 16S rRNA pyrosequencing. PLoS One 9, e103115.

Ding, J., Li, F., Yang, G., Chen, L., Zhang, B., Liu, L., Fang, K., Qin, S., Chen, Y., Peng, Y., Ji, C., He, H., Smith, P., Yang, Y., 2016. The permafrost carbon inventory on the Tibetan Plateau: a new evaluation using deep sediment cores. Global Change Biology 22, 2688–2701.

Ding, W.-X., Cai, Z.-C., 2007. Methane emission from natural wetlands in China: summary of years 1995–2004 studies. Pedosphere 17, 475–486.

Dörfer, C., Kuhn, P., Baumann, F., He, J.S., Scholten, T., 2013. Soil organic carbon pools and stocks in permafrost-affected soils on the Tibetan Plateau. PLoS One 8, e57024.

Duddleston, K.N., Kinney, M.A., Kiene, R.P., Hines, M.E., 2002. Anaerobic microbial biogeochemistry in a northern bog: acetate as a dominant metabolic end product. Global Biogeochemical Cycles 16. http://dx.doi.org/10.1029/2001GB001402.

Dufrene, M., Legendre, P., 1997. Species assemblages and indicator species: the need for a flexible asymmetrical approach. Ecological Monographs 67, 345–366.

Freitag, T.E., Prosser, J.I., 2009. Correlation of methane production and functional gene transcriptional activity in a peat soil. Applied and Environmental Microbiology 75, 6679–6687.

Galand, P.E., Fritze, H., Conrad, R., Yrjala, K., 2005. Pathways for methanogenesis and diversity of methanogenic archaea in three boreal peatland ecosystems. Applied and Environmental Microbiology 71, 2195–2198.

Graham, D.E., Wallenstein, M.D., Vishnivetskaya, T.A., Waldrop, M.P., Phelps, T.J., Pfiffner, S.M., Onstott, T.C., Whyte, L.G., Rivkina, E.M., Gilichinsky, D.A., Elias, D.A., Mackelprang, R., VerBerkmoes, N.C., Hettich, R.L., Wagner, D., Wullschleger, S.D., Jansson, J.K., 2012. Microbes in thawing permafrost: the unknown variable in the climate change equation. ISME Journal 6, 709–712.

Hattori, S., 2008. Syntrophic acetate-oxidizing microbes in methanogenic environments. Microbes and Environments 23, 118–127.

Hirota, M., Tang, Y.H., Hu, Q.W., Hirata, S., Kato, T., Mo, W.H., Cao, G.M., Mariko, S., 2004. Methane emissions from different vegetation zones in a Qinghai-Tibetan Plateau wetland. Soil Biology and Biochemistry 36, 737–748.

Hodgkins, S.B., Tfaily, M.M., McCalley, C.K., Logan, T.A., Crill, P.M., Saleska, S.R., Rich, V.I., Chanton, J.P., 2014. Changes in peat chemistry associated with permafrost thaw increase greenhouse gas production. Proceedings of the National Academy of Sciences 111, 5819–5824.

IPCC, 2007. Climate change 2007: the physical science basis. In: Contribution of Working Group I to the Fourth Assessment Report of the Intergovernmental Panel on Climate Change. USA., Cambridge, United Kingdom and New York, NY, p. 996.

Jin, H., He, R., Cheng, G., Wu, Q., Wang, S., Lü, L., Chang, X., 2009. Changes in frozen ground in the source area of the Yellow River on the Qinghai-Tibet Plateau, China, and their eco-environmental impacts. Environmental Research Letters 4, 045206.

Jin, H.J., Wu, J., Cheng, G.D., Tomoko, N., Sun, G.Y., 1999. Methane emissions from wetlands on the Qinghai-Tibet Plateau. Chinese Science Bulletin 44, 2282–2286.

Keddy, P.A., 2010. Wetland Ecology: Principles and Conservation. Cambridge University Press, Cambridge, UK.

Kotsyurbenko, O., Friedrich, M., Simankova, M., Nozhevnikova, A., Golyshin, P., Timmis, K., Conrad, R., 2007. Shift from acetoclastic to H_2-dependent methanogenesis in a West Siberian peat bog at low pH values and isolation of an acidophilic *Methanobacterium* strain. Applied and Environmental Microbiology 73, 2344–2348.

Kotsyurbenko, O.R., 2005. Trophic interactions in the methanogenic microbial community of low-temperature terrestrial ecosystems. FEMS Microbiology Ecology 53, 3–13.

Liebner, S., Ganzert, L., Kiss, A., Yang, S., Wagner, D., Svenning, M.M., 2015. Shifts in methanogenic community composition and methane fluxes along the degradation of discontinuous permafrost. Frontiers in Microbiology 6, 356.

Liu, Y., Yao, T., Gleixner, G., Claus, P., Conrad, R., 2013. Methanogenic pathways,^{13}C isotope fractionation, and archaeal community composition in lake sediments and wetland soils on the Tibetan Plateau. Journal of Geophysical Research-Biogeosciences 118, 1–15.

Logares, R., Lindstrom, E.S., Langenheder, S., Logue, J.B., Paterson, H., Laybourn-Parry, J., Rengefors, K., Tranvik, L., Bertilsson, S., 2013. Biogeography of bacterial communities exposed to progressive long-term environmental change. ISME Journal 7, 937–948.

Ma, B., Wang, H., Dsouza, M., Lou, J., He, Y., Dai, Z., Brookes, P.C., Xu, J., Gilbert, J.A., 2016. Geographic patterns of co-occurrence network topological features for soil microbiota at continental scale in eastern China. ISME Journal 10, 1891–1901.

McCalley, C.K., Woodcroft, B.J., Hodgkins, S.B., Wehr, R.A., Kim, E.H., Mondav, R., Crill, P.M., Chanton, J.P., Rich, V.I., Tyson, G.W., Saleska, S.R., 2014. Methane dynamics regulated by microbial community response to permafrost thaw. Nature 514, 478–481.

McDonald, J.H., 2014. Handbook of Biological Statistics, third ed. Maryland, Sparky House Publishing, Baltimore.

McMurdie, P.J., Holmes, S., 2013. phyloseq: an R package for reproducible interactive analysis and graphics of microbiome census data. PLoS One 8, e61217.

McMurdie, P.J., Holmes, S., 2014. Waste not, want not: why rarefying microbiome

data is inadmissible. PLoS Computational Biology 10, e1003531.
Megonigal, J.P., Mines, M.E., Visscher, P.T., 2005. Anaerobic metabolism: linkages to trace gases and aerobic processes. In: Schlesinger, W.H. (Ed.), Biogeochemistry. Elsevier, Oxford, UK, pp. 350–362.
Mondav, R., Woodcroft, B.J., Kim, E.-H., McCalley, C.K., Hodgkins, S.B., Crill, P.M., Chanton, J., Hurst, G.B., VerBerkmoes, N.C., Saleska, S.R., Hugenholtz, P., Rich, V.I., Tyson, G.W., 2014. Discovery of a novel methanogen prevalent in thawing permafrost. Nature Communications 5, 3212.
Nozhevnikova, A.N., Kotsyurbenko, O.R., Simankova, M.V., 1994. Acetogenesis at low temperature. In: Drake, H.L. (Ed.), Acetogenesis. Chapman and Hall, New York, pp. 416–431.
Oksanen, J., Blanchet, F.G., Kindt, R., Legendre, P., Minchin, P.R., O'Hara, R.B., Simpson, G.L., Solymos, P., Henry, M., Stevens, H., Wagner, H., 2013. Vegan: Community Ecology Package. R package version 2.0-7. http://CRAN.R-project.org/package=vegan.
Prater, J.L., Chanton, J.P., Whiting, G.J., 2007. Variation in methane production pathways associated with permafrost decomposition in collapse scar bogs of Alberta, Canada. Global Biogeochemical Cycles 21, GB4004.
Roberts, D., 2016. Labdsv: Ordination and Multivariate Analysis for Ecology. R package version 1.8-0. https://CRAN.R-project.org/package=labdsv.
Rooney-Varga, J.N., Giewat, M.W., Duddleston, K.N., Chanton, J.P., Hines, M.E., 2007. Links between archaeal community structure, vegetation type and methanogenic pathway in Alaskan peatlands. FEMS Microbiology Ecology 60, 240–251.
Sachs, T., Giebels, M., Boike, J., Kutzbach, L., 2010. Environmental controls on CH_4 emission from polygonal tundra on the microsite scale in the Lena river delta, Siberia. Global Change Biology 16, 3096–3110.
Sakai, S., Imachi, H., Sekiguchi, Y., Tseng, I.C., Ohashi, A., Harada, H., Kamagata, Y., 2009. Cultivation of methanogens under low-hydrogen conditions by using the coculture method. Applied and Environmental Microbiology 75, 4892–4896.
Schloss, P.D., Westcott, S.L., Ryabin, T., Hall, J.R., Hartmann, M., Hollister, E.B., Lesniewski, R.A., Oakley, B.B., Parks, D.H., Robinson, C.J., Sahl, J.W., Stres, B., Thallinger, G.G., Van Horn, D.J., Weber, C.F., 2009. Introducing mothur: open-source, platform-independent, community-supported software for describing and comparing microbial communities. Applied and Environmental Microbiology 75, 7537–7541.
Sollinger, A., Schwab, C., Weinmaier, T., Loy, A., Tveit, A.T., Schleper, C., Urich, T., 2016. Phylogenetic and genomic analysis of Methanomassiliicoccales in wetlands and animal intestinal tracts reveals clade-specific habitat preferences. FEMS Microbiology Ecology 92 fiv149.
Thauer, R.K., Kaster, A.K., Seedorf, H., Buckel, W., Hedderich, R., 2008. Methanogenic archaea: ecologically relevant differences in energy conservation. Nature Reviews Microbiology 6, 579–591.
Tian, J.Q., Shu, C., Chen, H., Qiao, Y.C., Yang, G., Xiong, W., Wang, L., Sun, J.Z., Liu, X.Z., 2015. Response of archaeal communities to water regimes under simulated warming and drought conditions in Tibetan Plateau wetlands. Journal of Soils and Sediments 15, 179–188.
Wagner, D., Kobabe, S., Liebner, S., 2009. Bacterial community structure and carbon turnover in permafrost-affected soils of the Lena Delta, northeastern Siberia. Canadian Journal of Microbiology 55, 73–83.
Wagner, D., Liebner, S., 2009. Global warming and carbon dynamics in permafrost soils: methane production and oxidation. In: Margesin, R. (Ed.), Permafrost Soils. Springer, Berlin, pp. 219–236.
Wagner, D., Lipski, A., Embacher, A., Gattinger, A., 2005. Methane fluxes in permafrost habitats of the Lena Delta: effects of microbial community structure and organic matter quality. Environmental Microbiology 7, 1582–1592.
Wang, Z., Li, Z., Xu, M., Yu, G., 2016. River morphodynamics and stream ecology of the Qinghai-Tibet Plateau. CRC press/balkema, Leiden,The Netherlands.
Wei, Y.Q., Fang, Y.P., 2013. Spatio-temporal characteristics of global warming in the Tibetan Plateau during the last 50 years based on a generalised temperature zone - elevation model. PLoS One 8, e60044.
Wickham, H., 2009. ggplot2: Elegant Graphics for Data Analysis. Springer-Verlag, New York.
Wille, C., Kutzbach, L., Sachs, T., Wagner, D., Pfeiffer, E.-M., 2008. Methane emission from Siberian arctic polygonal tundra: eddy covariance measurements and modeling. Global Change Biology 14, 1395–1408.
Wu, Q.B., Hou, Y.D., Yun, H.B., Liu, Y.Z., 2015. Changes in active-layer thickness and near-surface permafrost between 2002 and 2012 in alpine ecosystems, Qinghai-Xizang (Tibet) Plateau, China. Global and Planetary Change 124, 149–155.
Yang, S., Liebner, S., Alawi, M., Ebenhöh, O., Wagner, D., 2014. Taxonomic database and cut-off value for processing *mcrA* gene 454 pyrosequencing data by MOTHUR. Journal of Microbiological Methods 103, 3–5.
Yang, Y.H., Fang, J.Y., Tang, Y.H., Ji, C.J., Zheng, C.Y., He, J.S., Zhu, B., 2008. Storage, patterns and controls of soil organic carbon in the Tibetan grasslands. Global Change Biology 14, 1592–1599.
Zhang, G., Tian, J., Jiang, N., Guo, X., Wang, Y., Dong, X., 2008. Methanogen community in Zoige wetland of Tibetan plateau and phenotypic characterization of a dominant uncultured methanogen cluster ZC-I. Environmental Microbiology 10, 1850–1860.
Zhang, Y., Wang, G., Wang, Y., 2011. Changes in alpine wetland ecosystems of the Qinghai-Tibetan plateau from 1967 to 2004. Environmental Monitoring and Assessment 180, 189–199.
Zhao, Z.L., Zhang, Y.L., Liu, L.S., Liu, F.G., Zhang, H.F., 2015. Recent changes in wetlands on the Tibetan Plateau: a review. Journal of Geographical Sciences 25, 879–896.
Zhou, Y.W., Guo, D.X., Qiu, G.Q., Cheng, G.D., Li, S.D., 2000. Geocryology in China. Science Press. Beijing (in Chinese).